Vapor–Liquid Equilibrium in the System Carbon Dioxide/Dimethyl Ether

Charles Y. Tsang[†] and William B. Streett*

School of Chemical Engineering, Cornell University, Ithaca, New York 14853

Vapor–liquid equilibrium in the system carbon dioxide/dimethyl ether has been studied at ten temperatures from 0.0 to 113.41 °C and pressures to 7.9 MPa. The mixture critical line has been located and is shown to be continuous in *P–T–X* space between the critical points of the pure components. The results are compared to earlier measurements and to the predictions of several two- and three-constant equations of state. The two-constant Peng–Robinson equation predicts phase compositions in good agreement with experiment.

Introduction

Among the promising methods for making transportation fuels from coal is gasification of coal to synthesis gas ($CO + H_2$) followed by catalytic conversion to liquid fuels. The production of methanol from coal or synthetic gas can be carried out with existing technology, and the use of methanol as a fuel or as an additive to gasoline has received wide attention. Methanol has several drawbacks, however, including toxicity, affinity for water, relatively low energy content, and incompatibility with some plastic components found in modern fuel systems (*1*). An attractive alternative is the conversion of methanol to gasoline. The Mobil Research and Development Corp. has developed a two-step catalytic process in which methanol is first converted to dimethyl ether (DME), followed by the conversion of DME to gasoline (*1*, *2*). Alternative processes in which synthesis gas is converted directly to DME, without the need to go through the methanol intermediate, are also under study. (Dimethyl ether, $(CH_3)_2O$, is sometimes called methyl ether or methyl oxide. Its triple-point temperature is −41.5 °C and its critical point is T_c = 126.9 °C, P_c = 5.27 MPa. It is used commercially as a refrigerant, a solvent, an extraction agent, and an aerosol propellent and as a fuel for welding, cutting, and brazing.)

The efficient design of coal conversion processes employing methanol and DME will clearly require phase equilibrium data for a variety of fluid mixtures containing methanol, DME, water, CO, CO_2, H_2, CH_4, and other light hydrocarbons. We have embarked on an experimental program to study the vapor–liquid equilibria of several important binary systems drawn from this group. The CO_2/DME system is the first to be studied in this program. Experiments on DME/methanol are in progress.

Experimental Method

The experimental method (*3*) is similar to that used in recent experiments on cryogenic systems, including H_2/CH_4 (*4*), H_2/CO_2 (*5*), and H_2/CO (*6*). For this work a new vapor-recirculating equilibrium system, designed for use at temperatures from 0 to 250 °C and pressures up to 200 MPa, has been constructed (Figure 1). Apart from the pump and the equilibrium cell, which were built in our laboratory, the equilibrium and sampling systems have been assembled from $^1/_8$-in. o.d. pressure tubing, with valves and fittings supplied by the High Pressure Equipment Co. (Erie, PA) and the Harwood Engineering Co. (Walpole, MA). The heart of the system is a continuous loop of high-pressure tubing, connecting an equilibrium cell H and a magnetic pump I, immersed in a liquid bath in thermostat M. After the temperature has been set, enough DME is added to fill the lower half of cell H (total volume $\simeq$ 10 cm^3) with liquid, and CO_2 is added to raise the pressure to the desired level. Equilibrium is established by the action of the magnetic pump I, which recirculates the vapor phase around the loop (in the direction shown by the arrows) and bubbles it through the liquid phase. The entire vapor phase passes through the liquid in a period of $\sim$1 min, ensuring a rapid approach to equilibrium. Analyses of samples withdrawn at different times have shown that equilibrium is established after 5–10 min of vapor recirculation under these conditions. The recirculating pump is similar to one described previously (*7*); however, the electromagnet that powered the earlier model has been replaced by three disk-shaped permanent magnets U_1, coupled to a small electric motor U_2 through a mechanical linkage V. The motor and the linkage produce a reciprocating motion in the magnets to drive the piston inside the pump. This change has been made to eliminate the heat load imposed on the bath by an electromagnet.

After equilibrium is reached, samples of the liquid and vapor phases are withdrawn through the capillary sampling lines J and K by opening valves P and Q. The vapor phase is sampled from the top of the pump I. The sampling lines and valves are heated by electrical tape from the exit of the bath to the entry into a heated sampling valve L. When the liquid sampling is throttled through the valve P, it vaporizes and enters L as a gas. The use of small-diameter tubing ($\sim$0.01-in. i.d.) in the sampling system keeps the dead volumes to a minimum and prevents physical separation of the components when vaporization occurs. The automatic gas sampling valve L is an integral part of the Hewlett-Packard Model 5840 gas chromatograph used for sample analysis in this work. When valve P or Q is opened, the sample flows through the sample chamber in L, purging it of all traces of the previous sample. The flow is monitored by a small flowmeter on the downstream side. When the analysis sequence of the gas chromatograph is initiated, mechanical action of the valve L places the sample chamber directly in the carrier stream.

Temperatures in the thermostat M are controlled to within ±0.02 °C by a Braun Model 1480 BKU proportional temperature controller TC through a temperature sensor TS and a heater TH and are measured with an accuracy of ±0.01 °C by an NBS-calibrated platinum resistance thermometer and a Mueller bridge (not shown). The temperature controller includes a pump for circulating the liquid in the thermostat (a mixture of water and ethylene glycol was used in this work). This is supplemented by an auxiliary stirrer ST. Subambient temperatures are obtained with an ice bath (0 °C) or by circulating cold water through an auxiliary coil in the thermostat. Pressures are measured with an accuracy of ±0.5% by means of an Autoclave Model DPS digital pressure gage G, calibrated in this laboratory against a Ruska dead-weight gage. Gas samples are analyzed with a Hewlett-Packard Model 5840 gas chromatograph with thermal conductivity detector. A 20-in. column of

[†] Pressent address: Texaco Canada Resources Ltd., Calgary, Alberta, Canada T2P 2P8.

0021-9568/81/1726-0155$01.25/0

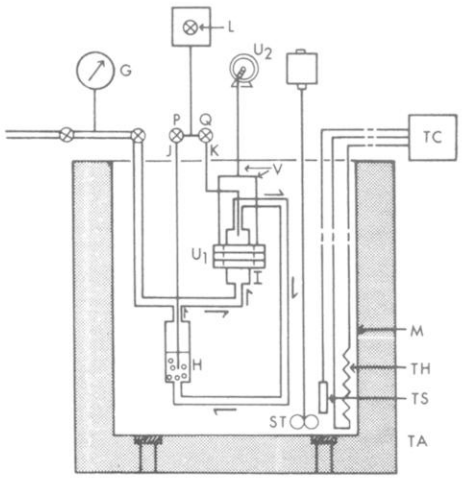

Figure 1. Schematic diagram of vapor-recirculating equilibrium system: (G) digital pressure gage; (H) pressure vessel containing vapor–liquid mixture; (I) magnetically operated pump for recirculating vapor; (J and K) sampling lines; (L) heated sampling valve in gas chromatograph; (M) thermostat; (P and Q) sampling valves; (ST) stirrer; (TA) stainless-steel tank; (TC) proportional temperature controller; (TH) heater; (TS) temperature sensor; (U_1) permanent magnets; (U_2) electric motor; (V) mechanical linkage.

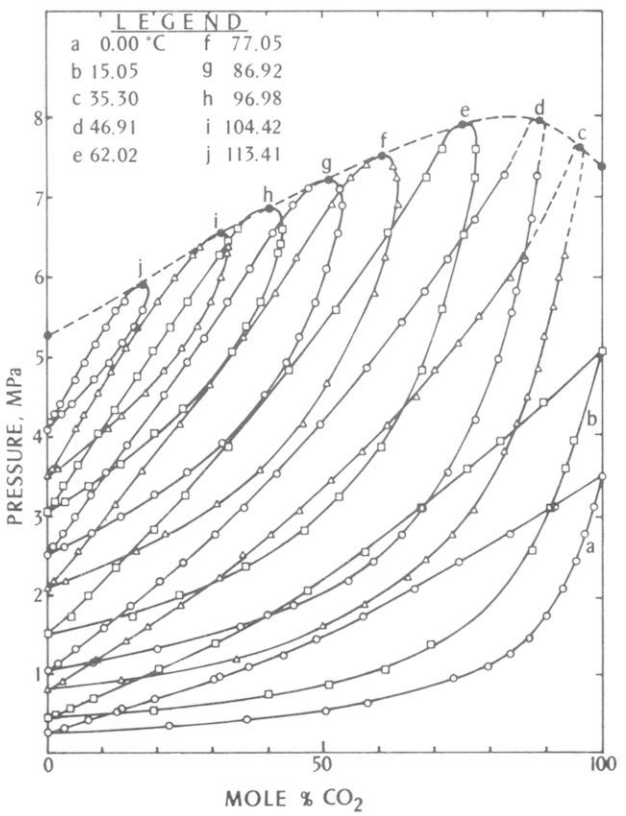

Figure 2. Experimental isotherms for CO_2/DME. The dashed line is the mixture critical line.

Poropack-Q was used, with helium carrier gas flowing at 25 cm^3/min. Because the response of the chromatograph is not linear over the entire composition range for CO_2/DME, it was calibrated against samples of known composition prepared in this laboratory. The analyses of gas samples are estimated to be accurate to within ±0.5 mol %. However, errors in the reported vapor and liquid compositions are due not only to errors in the analyses, but also to errors resulting from the sampling process. The maximum error in the phase compositions reported here, due to all causes, is estimated to be ±1.0 mol %, except near the critical line, where it may be as large as 2.0 mol %.

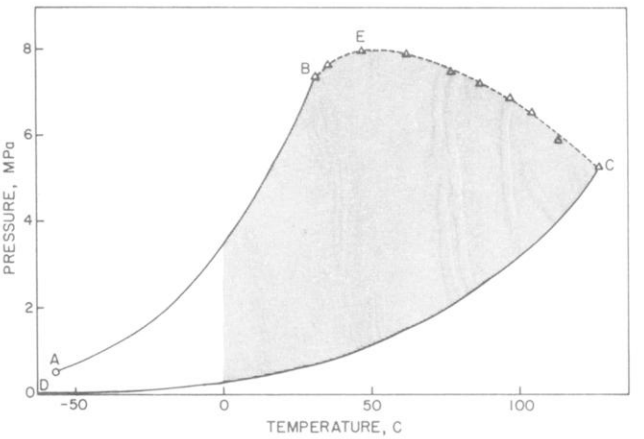

Figure 3. Pressure–temperature diagram. The shaded area is the $P-T$ region covered in this work. AB and DC are the vapor pressure curves of CO_2 and DME, and BEC is the mixture critical line.

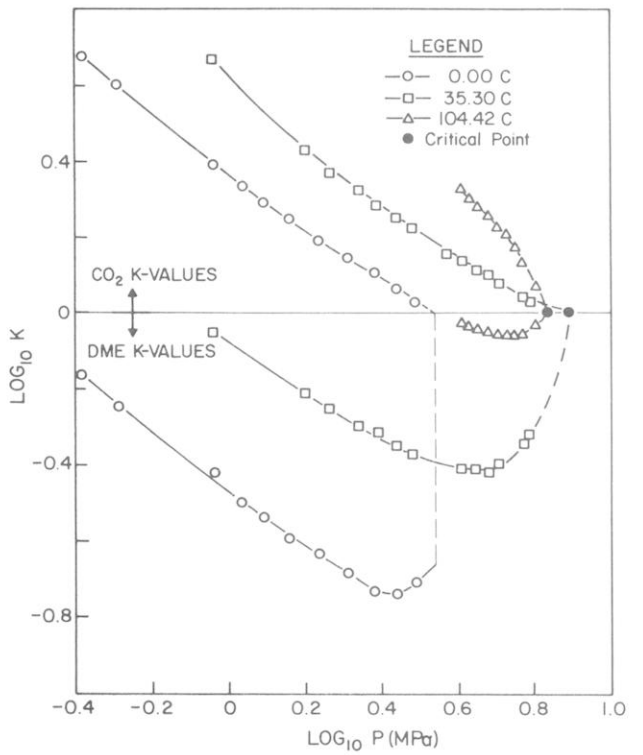

Figure 4. K values ($K \equiv Y/X$) for three typical isotherms in the CO_2/DME system.

Results

Vapor and liquid compositions have been measured at ten temperatures from 0.00 to 113.41 °C and pressures to 7.9 MPa. The data are recorded in Table I and plotted on a pressure–composition ($P-X$) diagram in Figure 2. The system exhibits negative deviations from Raoult's Law. The $P-T$ extent of the region covered by this study is shown as a shaded area in Figure 3. AB and DC are the vapor pressure curves of CO_2 and DME, respectively, with critical points B and C. BEC is the mixture critical line. Numerical data for the points on this line, obtained from large-scale graphs, are recorded in Table II. At temperatures of 62.02 °C and above, phase compositions were measured at pressures within ~0.2 MPa of the critical pressure; however, at 35.30 and 46.91 °C (isotherms c and d in Figure 2) the highest pressures at which phase separations were observed were ca. 1.4 and 0.7 MPa below the critical pressure. Precise control of the total composition of the mixture is required to obtain a phase separation in the narrow

Table I. Experimental Vapor-Liquid Compositions for CO_2/DME[a]

P, MPa	X_1	Y_1	P, MPa	X_1	Y_1
		T = 0.00 °C			
0.26	0.0000	0.0000	0.96	0.3109	
0.32	0.0309		1.09	0.3658	0.7959
0.34		0.2221	1.24	0.4286	0.8346
0.41	0.0763	0.3613	1.45	0.4877	0.8699
0.52	0.1270	0.5024	1.73	0.5722	0.9004
0.56	0.1354		2.07	0.6631	0.9300
0.62		0.5792	2.41	0.7445	0.9527
0.68	0.1965		2.76	0.8325	0.9694
0.92	0.3004		3.10	0.9149	0.9833
0.93		0.7334			
		T = 15.05 °C			
0.43	0.0000	0.0000	1.38	0.3016	0.6943
0.49	0.0169		1.74	0.3955	0.7793
0.54		0.1937	2.07	0.4708	0.8277
0.56	0.0403		2.55	0.5729	0.8733
0.69	0.0830		3.10	0.6788	0.9097
0.72		0.3992	3.59	0.7572	0.9345
0.85		0.5090	3.93	0.8140	0.9490
1.03		0.6104	4.41	0.8928	
1.05	0.2003				
		T = 35.50 °C			
0.79	0.0000	0.0000	3.45	0.5134	
0.85	0.0206		3.79	0.5695	0.8241
0.90	0.0291	0.1354	4.14	0.6141	0.8488
1.17	0.0891	0.3421	4.48	0.6597	0.8670
1.41	0.1447		4.83	0.7006	0.8857
1.59	0.1840	0.4987	5.17	0.7427	0.8962
1.86	0.2433	0.5743	5.52	0.7797	
2.21	0.3102	0.6528	5.63		0.9132
2.45	0.3535	0.6856	6.00	0.8375	0.9257
2.76	0.4055	0.7320	6.26	0.8611	0.9329
3.07	0.4568	0.7702			
		T = 46.91 °C			
1.05	0.0000	0.0000	4.15	0.4940	
1.14	0.0201	0.0864	4.19		0.7725
1.31	0.0528	0.2002	4.86	0.5781	
1.59	0.1023	0.3492	4.96		0.8128
1.86	0.1521	0.4472	5.43	0.6397	
2.17	0.2068	0.5437	5.54		0.8370
2.41	0.2494	0.5909	5.81	0.6828	0.8461
2.76	0.3035	0.6405	6.21	0.7222	0.8600
3.10	0.3576	0.6769	6.70	0.7714	0.8727
3.52	0.4154	0.7240	7.25	0.8242	0.8825
		T = 62.02 °C			
1.79	0.0448	0.1563	4.83	0.4361	0.6780
2.00	0.0756	0.2404	5.59	0.5216	0.7126
2.36	0.1254	0.3588	6.54	0.6130	0.7525
2.83	0.1930	0.4663	7.24	0.6845	0.7710
3.25	0.2499	0.5298	7.58	0.7126	0.7720
3.86	0.3286	0.6033	7.93	0.7364	0.7701
		T = 77.05 °C			
2.10	0.0000	0.0000	5.24	0.3550	
2.17	0.0112	0.0340	5.79	0.4137	0.5916
2.34	0.0312	0.0895	6.24	0.4508	0.6110
2.55	0.0553	0.1611	6.69	0.4900	0.6272
2.76	0.0797	0.2143	6.91	0.5168	0.6342
3.14	0.1231	0.3074	7.23		0.6318
3.57	0.1722	0.3879	7.26	0.5472	
4.15	0.2410	0.4652	7.38		0.6263
4.65	0.2955	0.5065	7.39	0.5795	
		T = 86.92 °C			
2.52	0.0000	0.0000	4.52	0.2135	0.3942
2.61	0.0104	0.0313	4.93	0.2531	0.4320
2.79	0.0296	0.0809	5.25	0.2850	0.4570
2.99	0.0502	0.1336	5.69	0.3269	0.4878
3.25	0.0787	0.1952	6.09	0.3652	0.5040
3.53	0.1082	0.2528	6.55	0.4093	0.5273
3.88	0.1426		6.90	0.4434	0.5351
3.91		0.3179	7.11	0.4734	0.5283
		T = 96.98 °C			
3.04	0.0000	0.0000	5.37	0.2268	0.3611
3.19	0.0134	0.0317	5.52	0.2376	0.3724
3.38	0.0317	0.0774	5.68	0.2546	0.3835
3.64	0.0564	0.1304	6.27	0.3119	
4.03	0.0923	0.1975	6.30		0.4177
4.34	0.1226	0.2462	6.41		0.4215
4.74	0.1634		6.43	0.3288	
5.05		0.3316	6.61	0.3460	0.4276
5.06	0.1928				
		T = 104.42 °C			
3.50	0.0000	0.0000	5.38	0.1692	0.2729
3.59	0.0101	0.0187	5.69	0.1996	0.2972
4.10	0.0523	0.1109	6.00	0.2311	0.3164
4.27	0.0679	0.1358	6.27	0.2631	
4.55	0.0932	0.1798	6.29		0.3260
4.83	0.1177	0.2127	6.37	0.2765	0.3288
5.10	0.1436	0.2429			
		T = 113.41 °C			
4.11	0.0000	0.0000	4.93	0.0684	0.1122
4.19	0.0060	0.0102	5.17	0.0888	0.1388
4.29	0.0146	0.0273	5.38	0.1064	0.1589
4.41	0.0251	0.0457	5.59	0.1243	0.1744
4.73	0.0508	0.0832	5.70	0.1417	

[a] X_1 is the mole fraction of CO_2 in the liquid, and Y_1 is the mole fraction of CO_2 in the vapor; DME vapor pressures are from ref *13*.

Table II. Vapor-Liquid Critical Line for CO_2/DME

temp, °C	press., MPa	composition, mol % CO_2
31.04[a]	7.39	100.0
35.30	7.7	96.0
46.91	8.0	88.0
62.02	7.9	76.0
77.05	7.5	60.5
86.92	7.2	50.5
96.98	6.9	40.5
104.42	6.6	33.5
113.41	5.9	15.0
126.90[b]	5.27	0.0

[a] Critical point of CO_2. [b] Critical point of DME.

portions of these isotherms. No special effort was made to explore this region in detail; hence, that portion of the critical line between 31.04 °C (the CO_2 critical temperature) and 62.02 °C is only qualitative.

Figure 4 is a plot of log K ($K \equiv Y/X$) vs. log P for three typical isotherms.

Comparison with Published Data

A literature search turned up only one previous study of this system, that of Winkler and Maass (*8*) in 1932. They used a static method in which dew and bubble points were measured for five known mixtures under different conditions of pressure and temperature. To obtain a dew point, they kept the pressure constant and raised the temperature until the last drop of liquid evaporated. On the other hand, they obtained bubble points by keeping the temperature constant and raising the pressure until the last bubble of vapor condensed. A typical comparison of their data with ours is shown in Figure 5, where measurements have been cross plotted on a T–X diagram at P = 5.5 MPa. Except for two of their vapor points, the agreement is very poor. We believe that these large discrepancies may be due to a failure to establish equilibrium in the pressure vessel of Winkler and Maass as the dew and bubble points were approached. They used a vessel of 500-mL volume, with no internal mixing or stirring, and located a bubble point by observing the disappearance of the last bubble of vapor at the top of the cell. Under these conditions, equilibrium between vapor

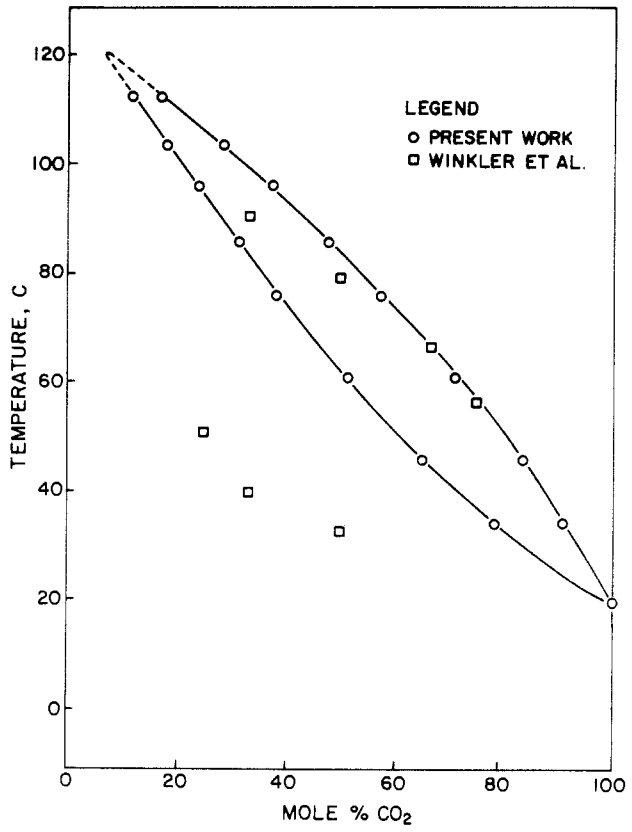

Figure 5. *T–X* comparison of the results of this work with published data of Winkler and Maass (*8*), at $P = 5.5$ MPa.

and liquid can be established only through diffusion—a slow process, especially in view of the large volume. A similar problem exists in the measurement of dew points, although it is probably less severe because of more rapid diffusion in the vapor phase than in the liquid.

Equation of State Calculations

Our experimental results have been compared to the predictions of three equations of state: the Redlich–Kwong (RK) equation (*9*), the Peng–Robinson (PR) equation (*10*), and the Deiters (DE) equation (*11*). The latter equation is a three-constant equation developed from a square-well intermolecular potential model and is based in part on the Carnahan–Starling equation (*12*). Details of the application of these equations to vapor–liquid equilibrium calculations have been published (*9–11*). Each equation contains an "energy" parameter a and a "volume" parameter b that are combined according to the following rules for applications to mixtures:

RK

$$a = a_{11}X_1^2 + 2a_{12}X_1X_2 + a_{22}X_2^2$$
$$b = b_{11}X_1^2 + 2b_{12}X_1X_2 + b_{22}X_2^2 \quad (1)$$

PR

$$a = a_{11}X_1^2 + 2a_{12}X_1X_2 + a_{22}X_2^2$$
$$b = b_{11}X_1 + b_{22}X_2 \quad (2)$$

DE

$$a = a_{11}X_1 + a_{22}X_2 + X_1X_2\Delta$$
$$b = b_{11}X_1^2 + 2b_{12}X_1X_2 + b_{22}X_2^2 \quad (3)$$

where a_{11}, a_{22}, b_{11}, and b_{22} are the pure component parameters, and a_{12} and b_{12} the cross parameters. The factor Δ in the DE equation includes the a_{12} parameter and other factors that account for nonrandomness and differences in size at the molecular level (*11*). The cross parameters are obtained in the usual way:

$$a_{12} = (1 - k_{12})a_{11}^{1/2}a_{22}^{1/2}$$
$$b_{12} = (1 - j_{12})(b_{11} + b_{22})/2 \quad (4)$$

where k_{12} and j_{12} are adjustable interaction parameters. To compare equation of state predictions to experiment, these interaction parameters were adjusted by trial and error to give the best fit to an isotherm in the middle range, 35.30 °C, and the results used to predict isotherms near the extremes of the experimental range (0.0 and 104.42 °C). The best values of the interaction parameters are recorded in Table III and the comparison is shown in Figure 6. At 35.30 °C and in the upper pressure range at 0.0 °C, predictions of the PR and DE equations are indistinguishable. These two equations are in good agreement with experiment and are clearly superior to the RK equation for this system. The PR equation is preferred over the DE equation on the basis of simplicity and ease of calculation. (The DE equation is designed for greater flexibility in treating complex molecular shapes and interactions and may well prove superior to the usual two-constant equations when applied to more complex systems.)

Table III. Interaction Parameters for the CO_2/DME System

	k_{12}	j_{12}
RK equation	−0.072	−0.113
PR equation	−0.020	
DE equation	0.005	−0.069

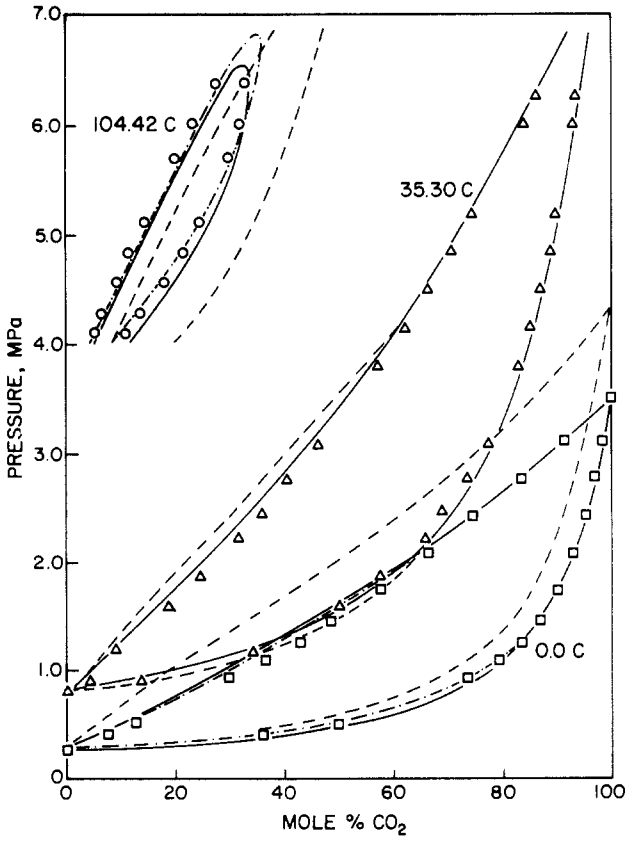

Figure 6. Comparison of experimental results with equation of state predictions: (O, Δ, □) experimental data; (—) DE equation; (–·–) PR equation; (– – –) RK equation. At 35.30 °C, and in the upper pressure range at 0.0 °C, predictions of the PR and DE equations are indistinguishable.

Acknowledgment

We are indebted to U. Deiters for performing the calculations using the RK and DE equations of state.

Literature Cited

(1) Harney, B. M.; Mills, A. G. *Hydrocarbon Process.* **1980**, *59*, 67.
(2) Chang, C. D.; Silvestri, A. J. *J. Catal.* **1977**, *47*, 249.
(3) Streett, W. B.; Calado, J. C. G. *J. Chem. Thermodyn.* **1978**, *10*, 1089.
(4) Tsang, C. Y.; Clancy, P.; Calado, J. C. G.; Streett, W. B. *Chem. Eng. Commun.* **1980**, *6*, 365.
(5) Tsang, C. Y.; Streett, W. B. *Chem. Eng. Sci.*, in press.
(6) Tsang, C. Y.; Streett, W. B. *Fluid Phase Equilib.*, in press.
(7) Streett, W. B.; Erickson, A. L. *Phys. Earth Planet. Inter.* **1972**, *5*, 357.
(8) Winkler, C. A.; Maass, O. *Can. J. Res.* **1932**, *6*, 458.
(9) Joffe, J.; Zudkevitch, D. *Ind. Eng. Chem. Fundam.* **1966**, *5*, 455.
(10) Peng, D. Y.; Robinson, D. B. *Ind. Eng. Chem. Fundam.* **1976**, *15*, 159.
(11) Deiters, U. Ph.D. Thesis, Bochum University, West Germany, 1979; *Chem. Eng. Sci.*, in press.
(12) Carnahan, N. F.; Starling, K. F. *J. Chem. Phys.* **1969**, *51*, 635.
(13) Braker, W.; Mossman, A. L. "Matheson Gas Data Book", 5th ed.; The Matheson Co.: E. Rutherford, NJ, 1971.

Received for review August 11, 1980. Accepted January 5, 1981. This work was supported in part by a grant from the Mobil Research and Development Corp. and in part by grants CPE 78-23537 and CPE 79-09168 from the National Science Foundation.

Solubility of Chlorine in Benzene, Toluene, Ethylbenzene, *o*-, *m*-, and *p*-Xylenes, and 2-, 3-, and 4-Chlorotoluenes

Michael Lohse and Wolf-Dieter Deckwer*

Institut für Technische Chemie, Universität Hannover, 3000 Hannover 1, Federal Republic of Germany

The solubilities of chlorine were measured in benzene, toluene, ethylbenzene, *o*-, *m*-, and *p*-xylenes, and monochlorinated toluenes at temperatures from 15 to 75 °C. A standard titration technique was used. The temperature dependency of the solubilities follows van't Hoff's equation. The heat of solution varies from 31 kJ/mol for benzene to 17 kJ/mol for xylene.

Introduction

There are many industrially important reactions which are carried out in multiphase systems. In such reaction systems, solubilities are fundamental data which are urgently needed for reliable design and scale-up purposes. Among the reactions carried out in gas–liquid reactors, chlorinations are widespread. It is therefore surprising that only a few solubility data are available for chlorine in aromatic compounds and their chlorinated derivatives (*1–4*). This communication presents new data on the solubility of chlorine in benzene, toluene, *o*-, *m*-, and *p*-xylenes, ethylbenzene, and the monochlorinated toluenes.

Experimental Section

The chlorination of alkylated aromatic compounds and their chloroderivatives proceeds fairly slowly in the dark but is substantially accelerated by visible light. Therefore, the measurements were carried out under conditions which prevented access of light, and, in addition, ~1% of phenol was added as an inhibitor.

The solubilities of chlorine were measured in a stirred cell, the design of which is shown in Figure 1. The all-glass cylindrical vessel had 6-cm i.d. and a height of 11 cm. It was enclosed in a thermostatic jacket and equipped with a reflux condenser, a gas inlet, and a sample tube. The whole vessel was wrapped in aluminum foil to suppress photochemical chlorination. Chlorine was taken from a cylinder and dried with sulfuric acid before being sparged into the liquid in the vessel. After the chlorine was sparged for 0.5 h under vigorous stirring, saturation was completed. Liquid samples were withdrawn by means of a sampling tube connected to the vessel (see Figure 1).

The chlorine content was analyzed by an iodine-displacement method similar to that used by Silberstein (*3*) and Le Page (*5*). The sample was injected into a certain volume of the corresponding aromatic, and then 250 mL of 0.5 N KI solution was added to the diluted sample. The liberated iodine is titrated with a standardized solution of $Na_2S_2O_3$.

The chlorine solubility in mol/L at a partial pressure of chlorine of 760 torr is calculated from eq 1, where N is the normality of $Na_2S_2O_3$ solution, V_T is the volume of $Na_2S_2O_3$ solution added, V_S is the sample volume, and P_{Cl_2} is the partial pressure of Cl_2 which is given by the barometric pressure P_B and the partial pressure of the solvent P_S; i.e.

$$c = \frac{NV_T}{2V_S}\frac{760}{P_{Cl_2}} \quad (1)$$

$$P_{Cl_2} = P_B - P_S \quad (2)$$

Results

The measured chlorine solubilities in the various aromatics for the temperature range of 15–75 °C are listed in Table I. Each value represents an average of three or four measurements. The mean relative error is less than 0.5%.

In Figures 2 and 3, log c is plotted vs. $1/T$. Straight lines were found; hence, the solubility of chlorine in the aromatics applied obeys van't Hoff's equation, i.e.

$$\log \frac{c(T_2)}{c(T_1)} = \frac{\Delta_S H}{2.303R}\left(\frac{1}{T_1} - \frac{1}{T_2}\right) \quad (3)$$

The heats of solution were obtained from least-squares fits and are given in Table I. The value of $\Delta_S H$ for toluene found in this study is in fair agreement with that of −23 kJ/mol assumed by Shah (*6*). Figure 4 compares the results of this study with data available from the literature. In the case of benzene, the

0021-9568/81/1726-0159$01.25/0